Acta of Bioengineering and Biomechanics
Vol. 18, No. 1, 2016

Original paper
DOI: 10.5277/ABB-00306-2015-03

Effects of the microcrack shape, size and direction on the poroelastic behaviors of a single osteon: a finite element study

HAI-PENG CEN[1], XIAO-GANG WU[1]*, WEI-LUN YU [1], QIU-ZU LIU[2], YUE-MEI JIA[1]

[1] Shanxi Key Laboratory of Material Strength & Structural Impact, and College of Mechanics, Taiyuan University of Technology, Taiyuan 030024, P.R. China.
[2] College of Mechanical Engineering, Taiyuan University of Technology, Taiyuan 030024, P.R. China.

Purpose: In this work, a finite element study is proposed by using the Comsol Multiphysics software to evaluate the effects of microcrack shape, size and direction on the poroelastic behaviors of a single osteon. *Methods*: This finite element model is established by using the Comsol Multiphysics software, and we just focus on the comparison of the influences of those microcrack geometric parameters on the osteonal fluid pressure and velocity. *Results*: The results show that: (1) microcracks in the osteon wall can induce a release of the fluid pressure, but enlarge the velocity in this region; (2) equal-area microcrack with ellipsoid-like shape produced a larger fluid pressure and velocity fields in the osteon than that of rectangular shape; (3) in the elliptic microcracks, the longer of the length (major semi-axis) induces a smaller fluid pressure and velocity amplitudes, whereas the width (minor axis) has little effect; (4) the direction of the microcracks (major axial direction) has an limited influence area around about 1/15 of the osteon cross-sectional area. *Conclusions*: This model permits the linking of the external loads and microcracks to the osteonal fluid pressure and velocity, which can be used for other purpose associate microcracks with the mechanotransduction and bone remodeling.

Key words: *osteon, poroelasticity, microcrack, finite element*

1. Introduction

Daily activities will induce a certain amount of fatigue microcracks in bone and interstitial fluid flow through among them. It is well known that microcrack is considered to be an important stimulus in the bone remodeling. The accumulation of lots microcracks will increase the risk of bone fractures and damage [2], [4], [5], [7], [12], [13], [20]. Therefore, the effects of microcracks on the bone fluid flow especially in an osteon should be addressed. Due to the limitations of technology, there is no direct experimental method to detect interstitial fluid flow in the osteon [3]. Thus, theoretical and numerical methods have been preferred.

Microcrack has its geometric features, such as shape, size and direction. These geometric parameters may influence the fluid pressure and velocity distribution in a loaded osteon. However, related research is scarce. Some focus on the influence of aging [12]: with the increasing of age, the microcrack in femoral compact bone was increased dramatically with an exponential function of growth trend, and the accumulation of microcracks will contribute to decrease bone strength and stiffness. Microcracks are various due to the anisotropic properties of bone. Under torsional loading [11], rat tibia with a circumferential microcrack is more severely damaged than that of a radial microcrack. A quarter 2D osteon model [14] is proposed by using Abaqus software to examine the propagation of fatigue mi-

* Corresponding author: Xiao-Gang Wu, Shanxi Key Laboratory of Material Strength & Structural Impact, and College of Mechanics, Taiyuan University of Technology, No.79, Street Yinze, Taiyuan 030024, China. Phone number: +86-351-6014477, e-mail: wuxiaogangtyut@163.com

Received: February 13th, 2015
Accepted for publication: April 17th, 2015

crocracks. The osteon is considered as a hollow cylinder and disregard the Haversian canal and the porosity. The results showed an initial crack propagation into the interstitial matrix, orthogonal to the load direction, but a certain deviation in the direction of the Haversian canal and arrest at the cement line. Moreover, the cement line strongly affects the crack path, like a barrier to prevent crack propagation and to cause a deviation. In this model, the fluid in the porosity is not considered, thus, a computational fluid dynamic model [5] of cortical bone is developed to evaluate the effect of a fatigue microcrack on the fluid flow field. The results show the presence of a fatigue microcrack that can alter velocity distribution as far as 150 μm away in its region, as well as has a potential to influence the fluid shear stress. In the above models, the poroelastic properties of the bone are not taken into account. Therefore, in order to well understand the mechanism of the mechanotransduction in bones especially in osteons, we have carried out a series of examinations of the poroelastic behaviors of osteon [15]–[19]. The effects of boundary conditions [15] and the material parameters [18] on the poroelastic behaviors of a single osteon have been examined in detail.

Recently, a microcracked osteon model [19] has been proposed by using the Comsol multiphysics software to examine the effects of microcracks on the poroelastic behaviors of an axial loaded osteon. In this model, the solid matrix and the fluid phase are treated as transverse isotropic poroelastic material and compressible liquid, respectively. Results show that the microcrack in the osteon wall can modify its local fluid pressure and velocity. In this paper, the effects of microcrack shape (ellipse and rectangle), size (length and width) and direction (from radial to circumferential) will be investigated. In particular, we will focus on the comparison of the influences of those geometric parameters on the osteonal fluid pressure and velocity.

2. Finite element model description

2.1. Geometry, boundary and material parameters

According to the previous studies [15]–[19], the osteon is also described as a hollow annular cylinder with cyclic and uniform loads applied in the longitudinal direction. As shown in the left of Fig. 1, a = 50 μm, b = 150 μm and h = 1 mm are inner (Haversian canal surface) radius, outer radius (cement surface), and height, respectively. The microcrack is presented in the osteon wall and its longitudinal axis of the microcrack is assumed to be perfectly aligned with z-axis. As shown in the right of Fig. 1, l and m are microcracks' length and width, respectively.

According to [19], the pore pressure in the Haversian canal and its surface is assumed to be null and the solid surface to be stress-free. The cement surface of the osteon is supposed to be impermeable and the displacement is constrained [9], [15], [19], but the

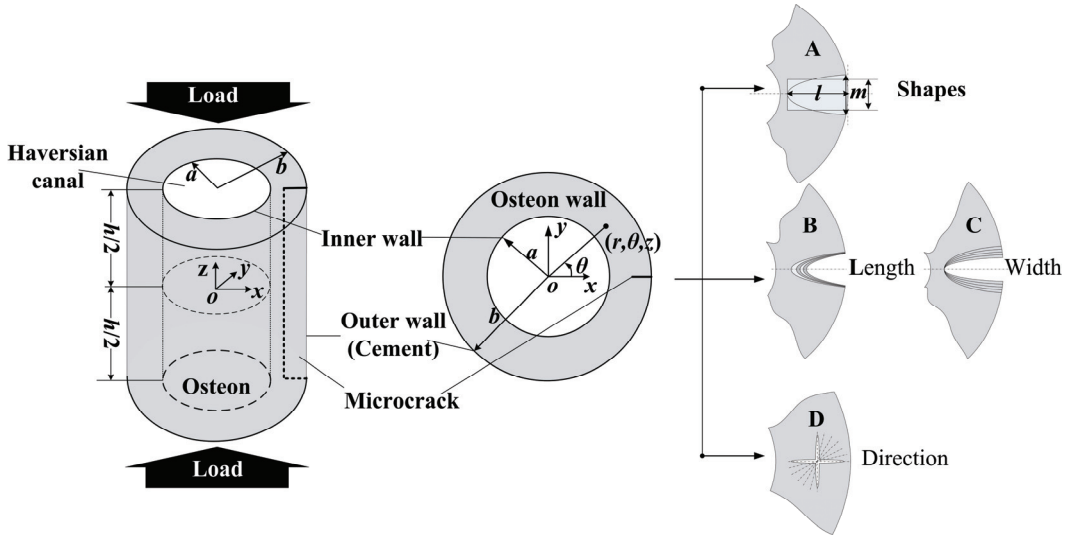

Fig. 1. Schematic microcracks in osteon model. A: two kinds of microcracks are imposed, one is rectangular and the other is elliptic; B and C: two geometrical parameters l and m are examined; D: Angles between the major axis and x-axis from the radial 0° to circumferential 90°

Table 1. Material constants used in the finite element model
[9], [14]–[16], [19]

C_{11} (GPa)	C_{12} (GPa)	C_{13} (GPa)	C_{33} (GPa)	C_{55} (GPa)	α
19.83	5.82	6.92	23.76	6.9	0.132
k (m^2)	μ (Pa s)	ρ_s ($Kg{\cdot}m^{-3}$)	ρ_f ($Kg{\cdot}m^{-3}$)	ϕ	C_p (1/Pa)
10^{-20}	10^{-3}	2000	1000	0.05	4e-10

pressure in cracked cement surface is zero and this surface allows fluid passage through freely. The imposed mechanical loadings on the top and bottom of the osteon are both represented by a harmonic displacement (w) of amplitude 0.5 μm and a frequency f, which leads to the maximum strain loading $\varepsilon = 0.001$ at 0.5 s, but the maximum pressure and velocity responses are at 0.25 s [19]:

$$w|_{z=\pm 0.5\text{mm}} = \pm 0.00025[\cos(2\pi f t) - 1][\text{mm}]. \quad (1)$$

In this work, the model is also established and analyzed by using the Comsol Multiphysics software (Version 4.3a). The material parameters for this FE model are grouped in Table 1 [19].

2.2. Goals and mash parameters

2.2.1. Goal 1: the shape

As shown in Fig. 1A, in order to examine the effect of microcrack's shape on the osteonal poroelastic response, two kinds of microcracks are imposed, one is rectangular and the other is elliptic. The length and width of rectangular microcrack are l = 15 μm, $m = \pi/10$ μm, and the major semi-axis and minor axis of the ellipse are l = 15 μm and m = 0.4 μm respectively. Thus they are equal-area. The mash parameters are grouped in Table 2.

Table 2. Elements and degrees used in goal 1

Shape	Elements	Degrees of freedom
Non-cracked	10 592	64 596
Rectangular	48 724	283 292
Ellipsoid-like	54 889	320 076

2.2.2. Goal 2: the size

As shown in Fig 1B and C, in order to evaluate the role of elliptic microcrack's size on the osteonal poroelastic behavior, two geometrical parameters l and m are examined. In the first case, m is fixed. The mash parameters are grouped in Table 3.

Table 3. Elements and degrees used in goal 2 for fixing m

l, m (μm)	Elements	Degrees of freedom
l = 5, m = 0.4	40 831	241 652
l = 15, m = 0.4	48 724	283 292
l = 25, m = 0.4	52 573	303 276
l = 35, m = 0.4	72 885	415 676
l = 45, m = 0.4	73 882	422 796

In the second case, l is fixed. The mash parameters are grouped in Table 4.

Table 4. Elements and degrees used in goal 2 for fixing l

l, m (μm)	Elements	Degrees of freedom
l = 15, m = 0.4	48 724	283 292
l = 15, m = 0.6	48 883	284 176
l = 15, m = 0.8	49 045	285 028
l = 15, m = 1.0	48 559	282 400
l = 15, m = 1.2	48 298	281 004

2.2.3. Goal 3: the direction

As shown in Fig. 1D, in order to evaluate the effect of microcrack's direction on the osteonal fluid flow behavior, 7 directions (angles between the major axis and x-axis from the radial direction 0° to circumferential direction 90°) are proposed in the elliptic microcracked osteon model. The elliptic microcracks' central point, l and m are fixed at (135 μm, 0, 0), l = 15 μm and m = 0.4 μm, respectively. The mash parameters are grouped in Table 5.

Table 5. Elements and degrees used in goal 3

Directions	Elements	Degrees of freedom
0°	192 425	1 093 292
15°	198 234	1 135 584
30°	202 148	1 159 220
45°	205 958	1 181 596
60°	250 568	1 429 024
75°	251 512	1 435 264
90°	187 225	1 068 640

3. Result

3.1. Effect of the microcracked shape

The finite element method has been validated in the previous study [19], and results are presented at $t = 0.25$ s corresponding to the maximum compression effect [19]. In order to evaluate the effect of microcrack's shape on the osteonal poroelastic behavior, the radial distribution of the pressure (Fig. 2A) and velocity amplitudes (Fig. 2B) in different microcrack shaped (None microcrack, Elliptic microcrack, rectangular microcrack) osteon model are plotted. As shown in Fig. 2, the pressure (P) and velocity (v) amplitudes in non-microcracked osteon model present an axial symmetrical distribution. Non-microcracked osteon model has a larger pressure distribution on the cracked region side but smaller velocity distribution on the opposite side. The pressure and velocity amplitudes in osteon with elliptic shape microcrack is larger than that of rectangular shape. The pressure peaks at $r = 101$ μm are 13.2 kPa and 12.5 kPa for these two shapes, respectively, and the velocity peaks at the microcrack origin point $r = 135$ μm are 2.81×10^{-7} m/s and 2.63×10^{-7} m/s. Thus, they are present at different points, but it is noted that

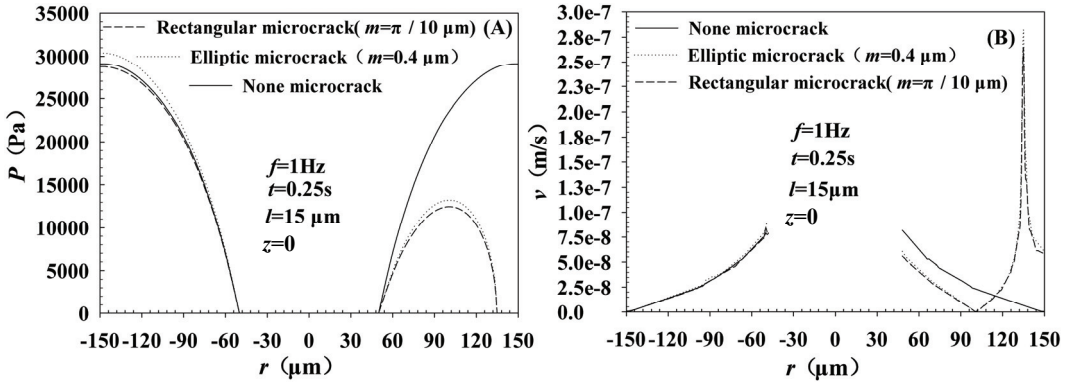

Fig. 2. Radial distribution of pressure (P, A) and velocity (v, B) amplitudes in different microcrack shaped (none microcrack, elliptic microcrack, rectangular microcrack) osteon

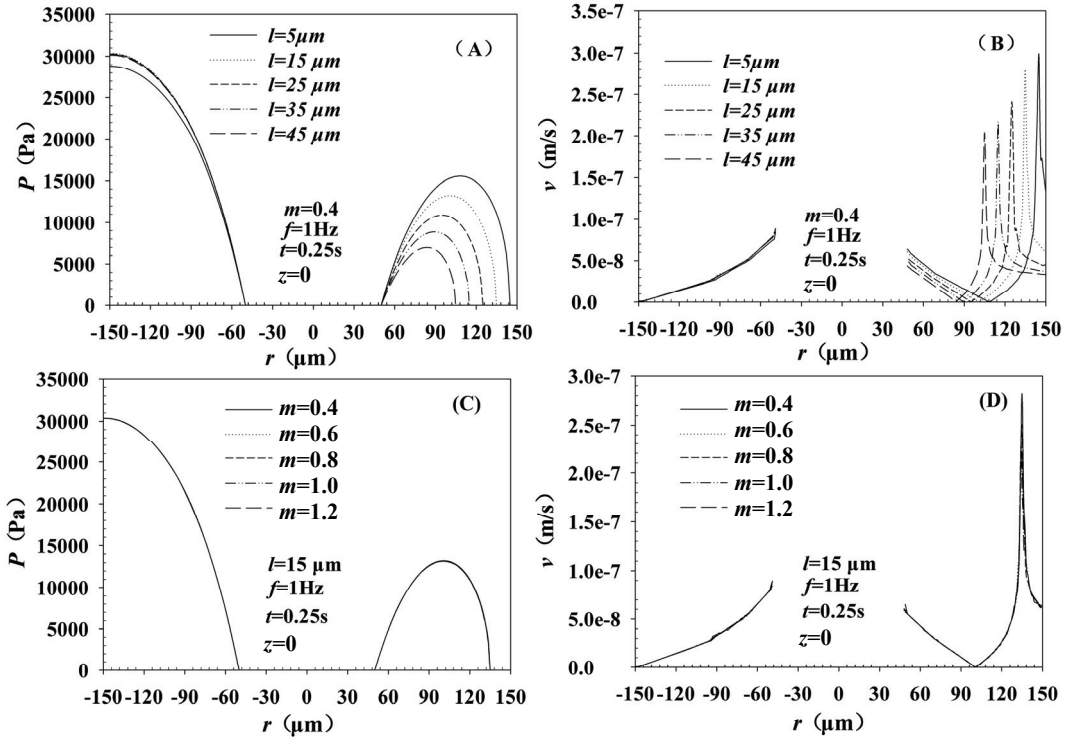

Fig. 3. Radial distributions of pressure (A, C) and velocity amplitudes (B, D) in microcracked osteon with different cracked (A, B: $m = 0.4$ μm, $l = 5$ μm, 15 μm, 25 μm, 35 μm, 45 μm) and width (C, D: $l = 15$ μm, $m = 0.4$ μm, 0.6 μm, 0.8 μm, 1.0 μm, 1.2 μm)

the pressure peak point (at r = 101 μm) is the same point with the minimum value (nearly zero) of the velocity.

3.2. Effect of the microcracked size

Ageing or intensity of bearing loads can cause the spread of the osteonal microcracks, especially in their length or width directions [12]. In order to evaluate the effect of microcrack size on the poroelastic behavior of osteon, the radial distributions of the pressure (Fig. 3A, 3C) and velocity amplitudes (Fig. 3B, 3D) in microcracked osteon with different cracked length (Fig. 3(A) and (B): m = 0.4 μm, l = 5 μm, 15 μm, 25 μm, 35 μm, 45 μm) and width (Fig. 3C and D: l = 15 μm, m = 0.4 μm, 0.6 μm, 0.8 μm, 1.0 μm, 1.2 μm) microcracks are plotted, respectively. As shown in Fig. 3(A), the pressure amplitude in l = 5 μm case is 28.8 kPa at r = –150 μm which is significantly smaller than the other cases. On the right side of the cracked osteon model and as shown in Fig. 3A and B, the pressure and velocity amplitudes decrease with the length growing. Pressure peaks for five cases are 15.6 kPa, 13.2 kPa, 10.9 kPa, 8.9 kPa and 7.0 kPa, and their own corresponding coordinates are at r = 108 μm, r = 101 μm, r = 95 μm, r = 90 μm and r = 84 μm, respectively. The velocity peaks are all at microcracked origin point. It is noted that the width of microcrack has little effect on the pressure and velocity amplitude distributions as shown in Fig. 3C and D.

3.3. Effect of the microcracked direction

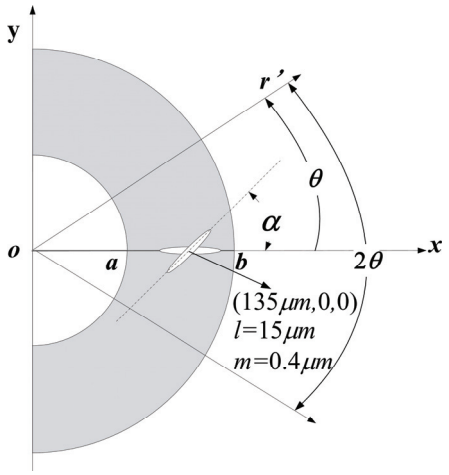

Fig. 4. The directions of microcacks: α is the angle between the major axis and x-axis from 0° to 90° (α = 0°, 15°, 30°, 45°, 60°, 75°, 90°). θ is the angle between the x-axis and normal axis r'

In order to evaluate the effect of microcrack direction on the poroelastic behavior of osteon, the radial distributions (r' as shown in Fig. 4, θ = ±4°, ±6°, ±8°, ±10°, ±12°, ±14°, ±16°, ±18°, ±20) of pressure (Fig. 5)

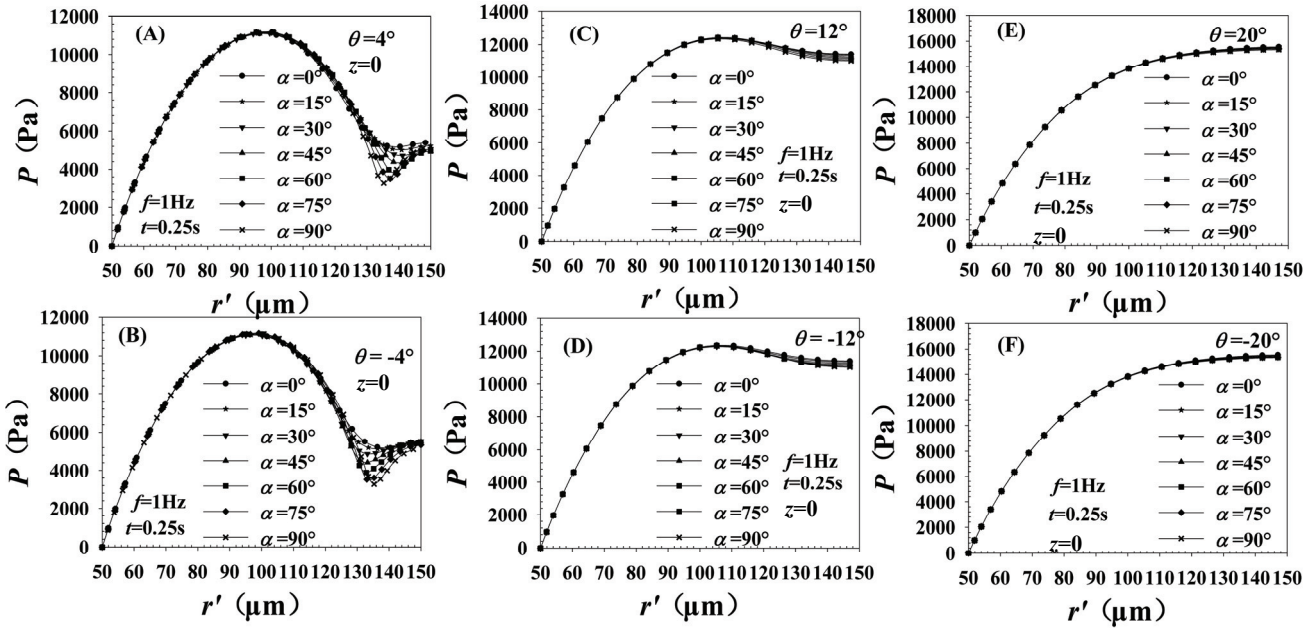

Fig. 5. Distributions of pressure amplitudes along the radial axis r' with different microcacked directions. (A): θ = 4°; (B): θ = –4°; (C): θ = 12°; (D): θ = –12°; (E): θ = 20°; (F): θ = –20°

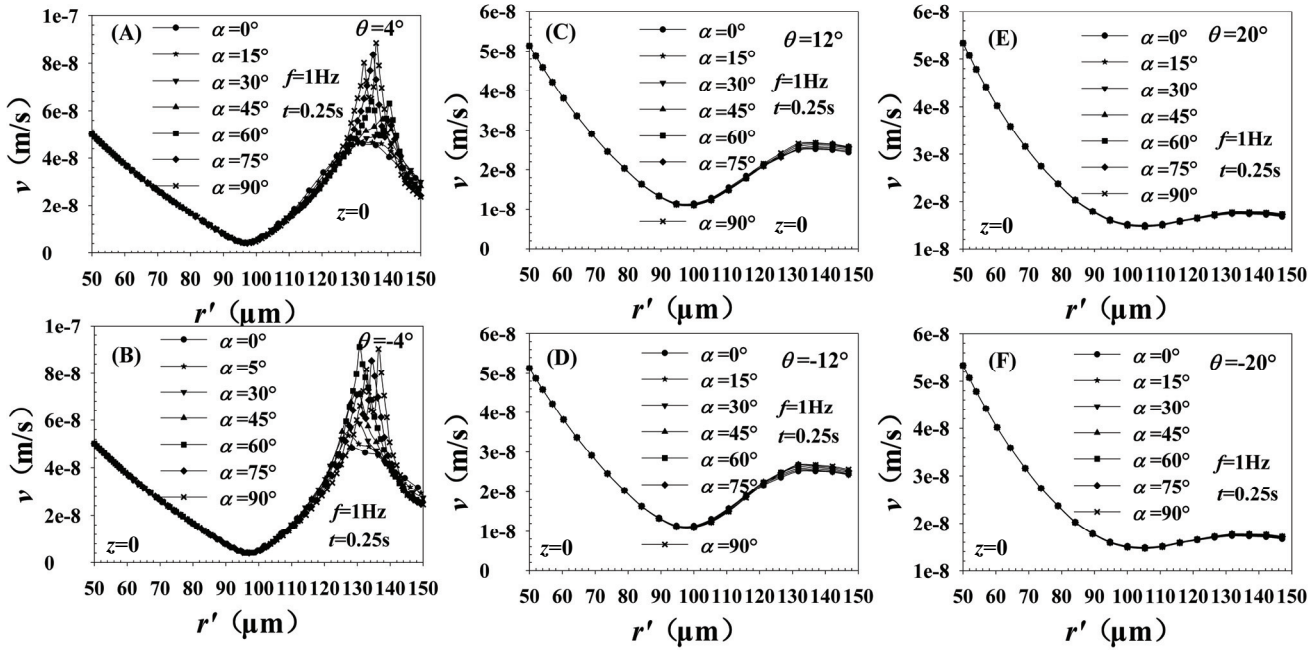

Fig. 6. Distributions of velocity amplitudes along the radial axis r' with different microcacked directions. (A): $\theta = 4°$; (B): $\theta = -4°$; (C): $\theta = 12°$; (D): $\theta = -12°$; (E): $\theta = 20°$; (F): $\theta = -20°$

and velocity (Fig. 6) amplitudes in microcracked osteon with different cracked directions ($\alpha = 0°$, 15°, 30°, 45°, 60°, 75°, 90°) are plotted. As shown in Fig. 5A and B and Fig. 6A and B, there is an "Affect Region" where the pressure and velocity amplitudes affected around the microcrack are about $|\theta| \leqslant 12°$. Once away from this region the distributions of pressure and velocity amplitudes show no obvious distinction. The fluid pressure increases/velocity decreases along the r' axis and there appears a peak/valley at $r' = 97.5$ μm/$r' = 96.5$ μm, then it begins to decrease/increase and enters into the "Affect Region" ($|\theta| \leqslant 12°$). Moreover, in this region the pressure valleys and velocity peaks present a grading regularity from $\alpha = 0°$ (radial direction) to $\alpha = 90°$ (circumferential direction).

4. Discussion

It is well known that fatigue microcracks occur in bone tissue due to the cyclic loading from daily activities and can immediately be repaired by bone remodeling. In this paper, finite element osteon models with different microcrack geometric parameters have been established under an axial harmonic loading by using the Comsol Multiphysics software. In this validated poroelastic FE model [19], the solid matrix and the fluid phase are treated as transverse isotropic and compressible, respectively. Moreover, this model permits the linking of the external loads and microcracks to the osteonal fluid pressure and velocity. In this work, we are just interest in examining the effects of microcrack shape, size and direction on the poroelastic responses of a loaded osteon, which may be a significant stimulus to the mechanotransduction of bone remodeling signals.

According to the boundary conditions imposed, the pressure amplitude in non-microcracked osteon model is supposed to be zero at r = 50 μm, and has a pressure peak at r = 150 μm, while the velocity varies oppositely. These results are in agreement with previous studies [19]. However, the fluid pressure and velocity amplitudes in cracked model both have an inflection point; one is the pressure peak, the other is the zero velocity point. It is noted that pressure peaks are produced in front of the microcrack starting point, while the velocity peak is just at that starting point. Compared with the non-microcracked osteon as shown in Fig. 2, the microcracks can induce a release of the fluid pressure, but enlarge the velocity in this region. This indicates that microcrack can release its region pressure and restrains the further damaging of osteon wall under the fatigue loading. Meanwhile, the increasing velocity around the microcracks accelerates the transporting of osteocyte's nutrients, metabolic waste and the chemical messengers, which could contribute to the processes of mechanotransduction and bone remodeling. This FE model and those results can also be used for proposing strategies that bone (cells) can sense the changes of surrounding mechanical environments associated with the mechanotransduction.

In fact, elliptic microcrack is more common than rectangular microcrack in the real microstructure of cortical bone [5], [8], [10]. However, researcher may establish the rectangular microcracks or damage [9], [19] to simplify the geometry and to reduce the computational costs. As a matter of fact, it is difficult for the osteon to have a rectangular microdamage in the physiological state. As shown in Fig. 3, where the fluid pressure and velocity amplitudes in different microcrack shaped osteon model are compared, the elliptic microcrack leads to a larger fluid pressure and velocity fields in the osteon than that of rectangular shaped microcrack. In this study, the pressure in microcrack is assumed to be zero and the microcrack break-through the cement surface of the osteon. However, some microcracks are passing through the osteon wall or stop at the cement line [14].

In this study, the pressure and velocity amplitudes decrease as the length grows, whereas the width of microcrack has little effect. In this case, the shorter microcrack may induce larger velocity amplitude and cause a larger fluid shear stress. It is widely believed that fluid flow-induced shear stress plays a major role in modulating the mechanotransduction process relevant to repairing the fatigue damage (remodeling) [1], [6]. Thus, that may be why the shorter microcrack has a faster repaired speed than the longer one.

In fact, osteonal microcracks are not uniform [8] and varied in the directions. There is a limited region around the microcack affected by the pressure and velocity amplitudes of the fluid. As shown in Fig. 5 and Fig. 6, with the increase of distance far from the microcrack, the effect on the fluid pressure and velocity amplitudes in the region becomes smaller and has no significant difference in $|\theta| \geq 12°$ (Fig. 5E and F and Fig. 6E and F). Circumferential ($|\alpha| = 90°$) and radial microcrack ($|\alpha| = 0°$) induced distributions of pressure and velocity amplitudes are significantly different. In order to examine the effect of damage on the bone stiffness loss under torsional loading, two kinds of microcracks [3] (circumferential and radial) are proposed. The circumferential microcrack will cause more damage potential than the radial one in the case of torsional loading [11]. Whereas, their model is elastic and ours is poroelastic, and we just focus on the effects of microcracks on the fluid pressure and velocity in the osteon.

5. Conclusion

In this paper, a finite element method is established by using the Comsol Multiphysics software to examine the effects of microcrack geometric features (shape, size and direction) on the poroelastic behaviors of a loaded osteon. This model can be used for other purpose associate microcracks with the mechanotransduction and bone remodeling. Though there are limitations in the study, some tentative conclusions are drawn below:

(1) Microcracks in the osteon wall can induce a release (decrease) of the fluid pressure, but enlarge the velocity in this region.
(2) Compared with the rectangular shaped microcrack, equal-area microcrack with ellipsoid-like shape produces a larger fluid pressure and velocity fields in osteon wall.
(3) In the elliptic microcrack and along its major axial direction, the longer of the major axis lengths induces a smaller fluid pressure and velocity amplitudes, whereas the length of the minor axis has little effect.
(4) The direction of the microcrack (major axial direction) has a limited influence area of about 1/15 of the osteon cross-sectional area.

Acknowledgement

This work was supported by the National Natural Science Foundation of China (No. 11302143), Natural Science Foundation of Shanxi (No. 2014021013), the Scientific and Technological Innovation Projects of Colleges and Universities in Shanxi Province (No. 2014116). The financial support from the Program for the Outstanding Innovative Teams of Higher Learning Institutions of Shanxi is also acknowledge.

References

[1] BAKKER A., KLEIN-NULEND J., BURGER E., *Shear stress inhibits while disuse promotes osteocyte apoptosis*, J. Biochemical and Biophysical Research Communications, 2004, 320, 1163–1168.
[2] BURR D.B., *The contribution of the organic matrix to bone's material properties*, J. Bone., 2002, 31, 8–11.
[3] CARDOSO L., FRITTON S.P., GAILANI G. et al., *Advances in assessment of bone porosity, permeability and interstitial fluid flow*, J. Biomechanics, 2013, 46, 253–265.
[4] DOBLARÉ M., GARCÍA J.M., GÓMEZ M.J., *Modelling bone tissue fracture and healing: a review*, J. Engineering Fracture Mechanics, 2004, 71, 217–238.
[5] GALLEY S.A., MICHALEK D.J., DONAHUE S.W., *A fatigue microcrack alters fluid velocities in a computational model of interstitial fluid flow in cortical bone*, J. Biomechanics, 2006, 39, 2026–2033.
[6] GOULETA G.C., HAMILTON N., COOPER D. et al., *Influence of vascular porosity on fluid flow and nutrient transport in loaded cortical bone*, J. Biomechanics, 2008, 41, 2169–2175.
[7] MCNAMARA L.M., PRENDERGAST P.J., *Bone remodeling algorithms incorporating both strain and microdamage stimuli*, J. Biomechanics, 2007, 40, 1381–1391.
[8] MOHSIN S., O'BRIEN F.J., LEE T.C., *Microcracks in compact bone: a three-dimensional view*, J. Anat., 2006, 209, 119–124.

[9] NGUYEN V.H., LEMAIRE T., NAILI S., *Anisotropic poroelastic hollow cylinders with damaged periphery under harmonically axial loadings: relevance to bone remodelling*, J. Multidiscipline Modeling in Materials and Structures, 2009, 5, 205–222.

[10] NGUYEN V.H., LEMAIRE T, NAILI S., *Influence of interstitial bone microcracks on strain-induced fluid flow*, J. Biomech Model Mechanobiol, 2011, 10, 963–972.

[11] PIDAPARTI R.M.V., *Microdamage simulation in a bone tissue using finite element analysis*, J. Elsevier Science Ltd., 1997, 3, 463–466.

[12] SCHAFFLER M.B., CHOI K., MILGROM C., *Aging and matrix microdamage accumulation in human compact bone*, J. Bone., 1995, 17, 521–525.

[13] STEPHEN C.C., *Bone poroelasticity*, J. Biomechanics, 1999, 32, 217–238.

[14] VERGANI L., COLOMBO C., LIBONATI F., *Crack propagation in cortical bone: a numerical study*, J. Procedia Materials Science, 2014, 3, 1524–1529.

[15] WU X.G., CHEN W.Y., *A hollow osteon model for examining its poroelastic behaviors: mathematically modeling an osteon with different boundary cases*, J. Mechanics/A Solids, 2013, 40, 34–49.

[16] WU X.G., CHEN W.Y., *Poroelastic behaviors of the osteon, a comparison of two theoretical osteon models*, J. Acta Mechanica Sinica, 2013, 29, 612–621.

[17] WU X.G., CHEN W.Y., GAO Z.P. et al., *The effects of Haversian fluid pressure and harmonic axial loading on the poroelastic behaviors of a single osteon*, J. Science China Physics, Mechanics & Astronomy, 2012, 55, 1646–1656.

[18] WU X.G., CHEN W.Y., WANG D.X., *A mathematical osteon model for examining its poroelastic behaviors*, J. Applied Mathematics and Mechanics, 2013, 34, 405–416.

[19] WU X.G., WANG Y.Q., WU X.H. et al., *Effects of microcracks on the poroelastic behaviors of a single osteon*, J. Science China Physics, Mechanics & Astronomy, 2014, 57, 2161–2167.

[20] YIN L., VENKATESAN S., WEBB D. et al., *Effect of cryo-induced microcracks on microindentation of hydrated cortical bone tissue*, J. Materials Characterization, 2009, 60, 783–791.